



# Politecnico di Bari

Repository Istituzionale dei Prodotti della Ricerca del Politecnico di Bari

A novel FDTD formulation based on fractional derivatives for dispersive Havriliak-Negami media

This is a pre-print of the following article

*Original Citation:*

A novel FDTD formulation based on fractional derivatives for dispersive Havriliak-Negami media / Bia, P.; Caratelli, D.; Mescia, L.; Cicchetti, R.; Maione, G.; Prudeniano, F.. - In: SIGNAL PROCESSING. - ISSN 0165-1684. - STAMPA. - 107:Feb. 2015(2015), pp. 312-318. [10.1016/j.sigpro.2014.05.031]

*Availability:*

This version is available at <http://hdl.handle.net/11589/884> since: 2021-03-09

*Published version*

DOI:10.1016/j.sigpro.2014.05.031

*Terms of use:*

(Article begins on next page)

# A novel FDTD formulation based on fractional derivatives for dispersive Havriliak–Negami media

P. Bia<sup>a</sup>, D. Caratelli<sup>b</sup>, L. Mescia<sup>a,\*</sup>, R. Cicchetti<sup>c</sup>, G. Maione<sup>a</sup>, F. Prudeniano<sup>a</sup>

<sup>a</sup>*Department of Electrical and Information Engineering, Politecnico di Bari, via E. Orabona 4 - 70125, Bari, Italy*

<sup>b</sup>*The Antenna Company Nederland B.V., Grebbeweg 111, 3911 AV, Rhenen, the Netherlands.*

<sup>c</sup>*Department of Information Engineering, Electronics and Telecommunications "Sapienza" University of Rome; Via Eudossiana, 18 - 00184 Rome, Italy*

---

## Abstract

A novel finite-difference time-domain (FDTD) scheme modeling the electromagnetic pulse propagation in Havriliak–Negami dispersive media is proposed. In traditional FDTD methods, the main drawback occurring in the evaluation of the electromagnetic propagation is the approximation of the fractional derivatives appearing in the Havriliak–Negami model equation. In order to overcome this problem, we have developed a novel FDTD scheme based on the direct solution of the time-domain Maxwell equations by using the Riemann–Liouville operator for fractional differentiation. The scheme can be easily applied to other dispersive material models such as Debye, Cole–Cole and Cole–Davidson. Different examples relevant to plane wave propagation in a variety of dispersive media are analyzed. The numerical results obtained by means of the proposed FDTD scheme are found to be in

---

\*Corresponding author

*Email address:* mescia@deemail.poliba.it (L. Mescia)

*URL:* <http://moe-group.poliba.it> (L. Mescia)

good accordance with those obtained implementing analytical method based on Fourier transformation over a wide frequency range. Moreover, the feasibility of the proposed method is demonstrated by simulating the transient wave propagation in slabs of dispersive materials.

*Keywords:*

Fractional derivatives, dispersive media, finite-difference time-domain (FDTD), biological tissues

---

## 1. Introduction

Recently, researches on the interaction between electromagnetic waves and biological tissues have received increasing attention due to their promising applications in the area of bioelectromagnetics. In fact, the application of electric field pulses has opened a new gateway to tumor treatment since their capability to induce significant morphological and functional changes in biological cells and tissues [1–6] as well as in molecular biology by promoting the understanding of molecular mechanisms of cells.

Despite substantial progress in experimental measurements in dielectric spectroscopy the modern state of the theory of dielectric relaxation remains unsatisfactory. The lack of data and accurate models, in wide frequency ranges, for complex dielectric properties of tissues has been an obstacle for both theoretical and experimental studies of electromagnetic field interaction with biological tissues. In fact, the various biological tissues in the human body are characterized by anomalies of the dynamic dielectric properties resulting in a strong dispersion of dielectric susceptibility. This dispersion, can be explained by considering that the disordered nature and microstructure

of the systems, the common property of fractal physiological structures and that power-law long-term memory effects yield a wide spectrum of relaxation times [7]. As result, the time-domain response is generally non-symmetric and markedly different from that of the simple Debye dielectrics.

It is well known that an accurate representation of the experimental dielectric response in frequency domain of complex biological tissues usually cannot be described by a simple exponential expression with a single relaxation time. At the present, a number of empirical relationships including Cole-Cole (CC), Cole-Davidson (CD) and Havriliak-Negami (HN) expressions have been proposed in order to fit such types of dielectric spectra. In particular, HN expression provides an extended model flexibility enabling a better parametrization of the dispersive media properties and a better description of the generalized broadened asymmetric relaxation loss peak.

Finite-difference time-domain (FDTD) method has been proven to be one of most powerful computational methods in electromagnetics to model the wave propagation in various complex media [8–10], such as biological materials. In particular, taking into account that the frequency-domain representation of the HN complex permittivity exhibits fractional powers of angular frequency  $j\omega$ , the conventional FDTD algorithm needs to be modified for implementing the approximation of fractional-order derivatives. Three major FDTD approaches have been proposed to simulate the time dependent propagation of electromagnetic waves in biological tissues: recursive convolution [11], auxiliary differential equation [12–16], and Z-transform [17–19]. In the recursive convolution approach, the convolution integral is discretized into convolution summation which is then evaluated recursively.

In auxiliary differential equation method the relative complex permittivity is approximated in the frequency domain by means of rational or polynomial functions leading to a number of ordinary differential equations. In the Z-transform approach, the time-domain convolution integral is reduced to a multiplication using the Z-transform. Alternative methods based on additional differential equation involving a fractional derivative have been proposed, too [11], [20]. However, the authors are unaware of any method in which the fractional operator regarding the most general HN response is directly incorporated in the FDTD scheme. To this aim, we present FDTD formulation based on Riemann-Liouville theory of fractional differentiation where the fractional derivatives are approximated using finite differences. Three types of dispersive media, described by CC, CD and HN expressions, are treated as special cases of our general formulation. Numerical results show that the proposed FDTD scheme leads to accurate simulations in a wideband frequency range.

## 2. Theoretical analysis

The Havriliak and Negami function is considered as a general expression for the universal relaxation law. As a consequence, the most general approximation for frequency dependence of the complex permittivity can be expressed by two-parameters formula

$$\epsilon_{r,HN}(\omega) = \epsilon_{r\infty} + \frac{\epsilon_{rs} - \epsilon_{r\infty}}{[1 + (j\omega\tau)^{1-\alpha}]^{1-\beta}} \quad (1)$$

where  $\epsilon_{rs}$  and  $\epsilon_{r\infty}$  are the static and infinite frequency dielectric constants, respectively,  $\tau$  is the relaxation time,  $0 \leq \alpha \leq 1$  and  $0 \leq \beta \leq 1$  are parameters which control the dispersion broadening. For  $\alpha = 0$  and  $\beta = 0$  eq. (1)

describes the well-known Debye model. Moreover, for  $\beta = 0$  and  $0 \leq \alpha \leq 1$  as well as for  $\alpha = 0$  and  $0 \leq \beta \leq 1$  the Cole–Cole and Cole–Davidson equations are obtained, respectively.

### 2.1. FDTD formulation

Ampere’s law in combination with the material relation in frequency domain can be written as

$$\begin{aligned}\nabla \times \mathbf{H} &= j\omega\epsilon_0\epsilon_{r\infty}\mathbf{E} + \mathbf{J} \\ &= j\omega\epsilon_0 \left( \epsilon_{r\infty} + \frac{\Delta\epsilon_r}{[1 + (j\omega\tau)^{1-\alpha}]^{1-\beta}} \right) \mathbf{E}\end{aligned}\quad (2)$$

where  $\Delta\epsilon_r = \epsilon_{rs} - \epsilon_{r\infty}$ , and  $\mathbf{J}$  is the polarization current

$$\mathbf{J} = \frac{j\omega\epsilon_0\Delta\epsilon_r}{[1 + (j\omega\tau)^{1-\alpha}]^{1-\beta}} \mathbf{E}. \quad (3)$$

Transforming (3) in time domain yields a fractional differential equation

$$(1 + \tau^{1-\alpha}\mathcal{D}_t^{1-\alpha})^{1-\beta} \mathbf{J} = D_t^{\alpha,\beta} \mathbf{J} = \epsilon_0\Delta\epsilon_r \frac{\partial \mathbf{E}}{\partial t} \quad (4)$$

where  $\mathcal{D}_t^{1-\alpha}$  is the  $(1 - \alpha)$ th-order fractional differential operator and

$$D_t^{\alpha,\beta} = (1 + \tau^{1-\alpha}\mathcal{D}_t^{1-\alpha})^{1-\beta}.$$

Based on the approximated binomial series, eq. (4) can be written as

$$D_t^{\alpha,\beta} \mathbf{J} \approx \sum_{n=0}^{N_{\alpha,\beta}} -\tau^{n(1-\alpha)} \binom{n + \beta - 2}{n} \mathcal{D}_t^{n(1-\alpha)} \mathbf{J}. \quad (5)$$

In order to choose the suitable value for  $N_{\alpha,\beta}$  ensuring the desired accuracy of the relative complex permittivity, eq. (1) has been taken into account to

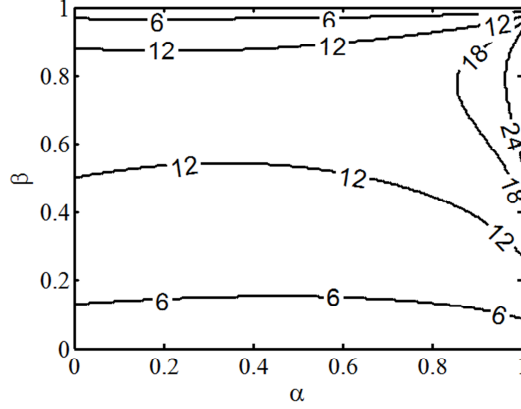


Figure 1: Number of terms  $N_{\alpha, \beta}$  of the binomial series approximation versus  $\alpha$  and  $\beta$  parameters.

write the truncated binomial series as follow

$$\underbrace{\left[1 + (j\omega\tau)^{(1-\alpha)}\right]^{1-\beta}}_{F(j\omega)} \approx \underbrace{\sum_{n=0}^{N_{\alpha, \beta}} (-1)^n \binom{n + \beta - 2}{n} (j\omega\tau)^{n(1-\alpha)}}_{F^a(j\omega)}$$

Fig. 1 shows the contour plot of  $N_{\alpha, \beta}$  versus both  $\alpha$  and  $\beta$  parameters considering as stop criterion the following error function

$$e_r = \sqrt{\sum_{\omega=0}^{\omega_{\max}} \left| \frac{F(j\omega) - F^a(j\omega)}{F(j\omega)} \right|^2} \leq 10^{-3}$$

By numerical simulation, a good approximation is obtained by using a number of terms lower then 6. However, the approximation accuracy can be improved by increasing the number of terms.

According to the popular Riemann-Liouville definition of fractional derivatives we derive

$$\mathcal{D}_t^{n(1-\alpha)} \mathbf{J} = \frac{d^\nu}{dt^\nu} \int_0^t \frac{(t-u)^{\nu-n(1-\alpha)-1}}{\Gamma(\nu-n(1-\alpha))} \mathbf{J} du \quad (6)$$

where  $\nu - 1 \leq n(1 - \alpha) < \nu$  and  $\Gamma(\cdot)$  is the gamma function. Moreover, by fixing

$$\mathbf{I}_{n,\alpha} = \int_0^t (t - u)^{\nu - n(1 - \alpha) - 1} \mathbf{J} \, du \quad (7)$$

and considering the central finite difference scheme with time step  $\Delta t$ , the eq. (7) evaluated at  $t = m\Delta t$  can be approximated by the sum

$$\left. \mathbf{I}_{n,\alpha} \right|^m \approx \sum_{p=0}^{m-1} \left. \mathbf{J} \right|^{m-p-\frac{1}{2}} \int_{p\Delta t}^{(p+1)\Delta t} u^{\nu - n(1 - \alpha) - 1} \, du \quad (8)$$

The  $\nu$ th-order time-derivative of  $\mathbf{I}_{n,\alpha}$  comparing in eq. (6) and calculated at the time instance  $t = m\Delta t$  can be approximated by the sum

$$\left. \frac{d^\nu \mathbf{I}_{n,\alpha}}{dt^\nu} \right|^m \approx \frac{1}{(\Delta t)^\nu} \sum_{p=0}^{\nu} (-1)^p \binom{\nu}{p} \left. \mathbf{I}_{n,\alpha} \right|^{m-p+1} \quad (9)$$

To get the electric field components, (4) is discretized at the time instant  $t = m\Delta t$

$$\left. \mathbf{E} \right|^{m+\frac{1}{2}} = \left. \mathbf{E} \right|^{m-\frac{1}{2}} + \frac{\Delta t}{\epsilon_0 \Delta \epsilon_r} \left. D_t^{\alpha,\beta} \mathbf{J} \right|^m \quad (10)$$

Moreover, applying finite difference scheme to the Ampere's law eq. (2) at the time instant  $t = m\Delta t$  we obtain

$$\left. \nabla \times \mathbf{H} \right|^m = \epsilon_0 \epsilon_{r\infty} \left. \frac{\partial \mathbf{E}}{\partial t} \right|^m + \left. \mathbf{J} \right|^m \quad (11)$$

where

$$\left. \mathbf{J} \right|^m = \frac{\left. \mathbf{J} \right|^{m+\frac{1}{2}} + \left. \mathbf{J} \right|^{m-\frac{1}{2}}}{2} \quad (12)$$

Using eqs. (4) (11) and (12), it is possible to derive the equation for updating the polarization current

$$\left. \mathbf{J} \right|^{m+\frac{1}{2}} = 2 \left. \nabla \times \mathbf{H} \right|^m - 2 \frac{\epsilon_{r\infty}}{\Delta \epsilon_r} \left. D_t^{\alpha,\beta} \mathbf{J} \right|^m - \left. \mathbf{J} \right|^{m-\frac{1}{2}} \quad (13)$$



Finally, by applying the finite difference scheme to the Faraday's law in the time domain, the updated magnetic field is given by

$$\mathbf{H} \Big|^{m+1} = \mathbf{H} \Big|^m - \frac{\Delta t}{\mu_0} \nabla \times \mathbf{E} \Big|^{m+\frac{1}{2}}. \quad (14)$$

## 2.2. UPML formulation

Let consider the electric field  $\mathbf{E}$  on the transverse  $x - y$  plane and propagating along the  $z$ -axis direction inside a 1D HN medium. To take into account the UPML boundary condition, the Maxwell equations are rewritten as follow:

$$\nabla \times \mathbf{H} = j\omega \bar{\bar{\mathbf{S}}} \mathbf{D} \quad (15)$$

$$\nabla \times \mathbf{E} = -j\omega \bar{\bar{\mathbf{S}}} \mathbf{B} \quad (16)$$

where

$$D_x = \epsilon_0 \epsilon_r s_z E_x \quad (17)$$

$$D_y = \epsilon_0 \epsilon_r E_y \quad (18)$$

$$B_x = \mu_0 s_z B_x \quad (19)$$

$$B_y = \mu_0 B_y \quad (20)$$

$$\bar{\bar{\mathbf{S}}} = \begin{pmatrix} 1 & 0 & 0 \\ 0 & s_z & 0 \\ 0 & 0 & 0 \end{pmatrix} \quad (21)$$

$$s_z = \kappa_z + \sigma_z / j\omega \epsilon_0 \quad (22)$$

and

$$\kappa_z(z) = \begin{cases} 1 & z \notin UPML \\ 1 + (\kappa_{MAX} - 1) \left( \frac{z - z_{UPML}^0}{d_{UPML}} \right)^m & z \in UPML \end{cases} \quad (23)$$

$$\sigma_z(z) = \begin{cases} 0 & z \notin UPML \\ \left( \frac{z - z_{UPML}^0}{d_{UPML}} \right)^m \sigma_{MAX} & z \in UPML \end{cases} \quad (24)$$

where  $z_{UPML}^0$  and  $d_{UPML}$  indicate the beginning and the thickness of the UPML.

Considering the eq.(15) it can be obtained the following expressions:

$$\frac{\partial H_y}{\partial z} = j\omega D_x \quad (25)$$

$$-\frac{\partial H_x}{\partial z} = j\omega s_z D_y \quad (26)$$

and, using eqs. (17) and (18), we derive the equations:

$$j\omega D_x = j\omega \epsilon_0 \epsilon_r s_z E_x \quad (27)$$

$$j\omega D_y = j\omega \epsilon_0 \epsilon_r E_y \quad (28)$$

Setting

$$J_x = \frac{j\omega \epsilon_0 \Delta \epsilon_r s_z}{[1 + (j\omega \tau)^{1-\alpha}]^{1-\beta}} E_x \quad (29)$$

$$J_y = \frac{j\omega \epsilon_0 \Delta \epsilon_r}{[1 + (j\omega \tau)^{1-\alpha}]^{1-\beta}} E_y \quad (30)$$

the eq. (25) and eq. (26) can be rewritten as:

$$\frac{\partial H_y}{\partial z} = j\omega \epsilon_0 \epsilon_{r\infty} s_z E_x + J_x \quad (31)$$

$$-\frac{\partial H_x}{\partial z} = j\omega \epsilon_0 \epsilon_{r\infty} s_z E_y + s_z J_y \quad (32)$$

Transforming eq. (29) and eq. (30) in time domain yields a fractional differential equations

$$D_t^{\alpha,\beta} J_x = \epsilon_0 \Delta \epsilon_r \kappa_z \frac{\partial E_x}{\partial t} + \Delta \epsilon_r \sigma_z E_x \quad (33)$$

$$D_t^{\alpha,\beta} J_y = \epsilon_0 \Delta \epsilon_r \frac{\partial E_y}{\partial t} \quad (34)$$

which are discretized at the time instant  $t = m\Delta t$  to get the electric field components:

$$E_x \Big|^{m+\frac{1}{2}} = \frac{2\epsilon_0 \kappa_z - \sigma_z \Delta t}{2\epsilon_0 \kappa_z + \sigma_z \Delta t} E_x \Big|^{m-\frac{1}{2}} + \frac{2\Delta t}{\Delta \epsilon_r (\epsilon_0 \kappa_z + \sigma_z \Delta t)} D_t^{\alpha,\beta} J_x \Big|^m \quad (35)$$

$$E_y \Big|^{m+\frac{1}{2}} = E_y \Big|^{m-\frac{1}{2}} + \frac{2\Delta t}{\Delta \epsilon_r \epsilon_0} D_t^{\alpha,\beta} J_y \Big|^m. \quad (36)$$

Using the eqs. (31)–(33) and (34) we obtain, in the time domain, the following expression:

$$\frac{\partial H_y}{\partial z} = \frac{\epsilon_{r\infty}}{\Delta \epsilon_r} D_t^{\alpha,\beta} J_x + J_x \quad (37)$$

$$-\frac{\partial H_x}{\partial z} = \frac{\epsilon_{r\infty}}{\Delta \epsilon_r} s_z D_t^{\alpha,\beta} J_y + s_z J_y \quad (38)$$

that can be used for updating the polarization current given by eq. (13).

Considering the eq.(16) and the constitutive relation (19) and (20), the updating equation for the magnetic field can be written as:

$$H_x \Big|^{m+1} = \frac{2\epsilon_0 \kappa_z - \sigma_z \Delta t}{2\epsilon_0 \kappa_z + \sigma_z \Delta t} H_x \Big|^m - \frac{B_x \Big|^{n+1} - B_x \Big|^n}{\mu_0 (2\epsilon_0 \kappa_z + \sigma_z \Delta t)} \quad (39)$$

$$H_y \Big|^{m+1} = H_y \Big|^m - \frac{B_y \Big|^{n+1} - B_y \Big|^n}{2\mu\epsilon_0} \quad (40)$$

where:

$$B_x \Big|^{m+1} = B_x \Big|^m - 2\epsilon_0 \Delta t \frac{\partial E_y}{\partial z} \Big|^{n+\frac{1}{2}} \quad (41)$$

$$B_y \Big|^{m+1} = \frac{2\epsilon_0 \kappa_z - \sigma_z \Delta t}{2\epsilon_0 \kappa_z + \sigma_z \Delta t} B_y \Big|^m + \frac{2\epsilon_0 \Delta t}{\mu_0 (2\epsilon_0 \kappa_z + \sigma_z \Delta t)} \frac{\partial E_x}{\partial z} \Big|^{n+\frac{1}{2}}. \quad (42)$$

### 3. Numerical Results

The proposed FDTD scheme has been validated by simulating the electromagnetic field propagation in three different biological media described by Cole–Cole, Cole–Davidson and Havriliak–Negami dielectric response. In Tab. 1 the material parameters used in the simulations are summarized.

Table 1: Parameters of the complex permittivity equation

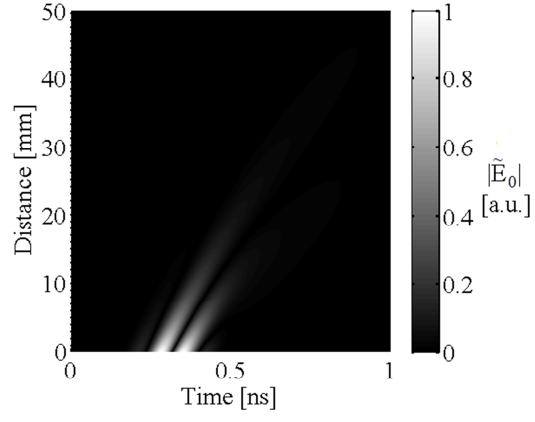
<b>Relation</b>	$\alpha$	$\beta$	$\tau$	$\epsilon_{rs}$	$\epsilon_{r\infty}$
Cole–Cole	0.3	0	153 ps	50	2
Cole–Davidson	0	0.15	153 ps	50	2
Havriliak–Negami	0.3	0.15	153 ps	50	2

To evaluate the accuracy of the proposed FDTD scheme a one-dimensional problem, where the dispersive region  $z \geq 0$  is surrounded by UPML, has been considered. The input source is a density current  $\mathbf{I}_s$  imprinted in a fixed point,  $z_0$ , inside the 1D computational domain and generating a x-axis polarized electric field. In particular, a modulated Gaussian pulse is used [13]:

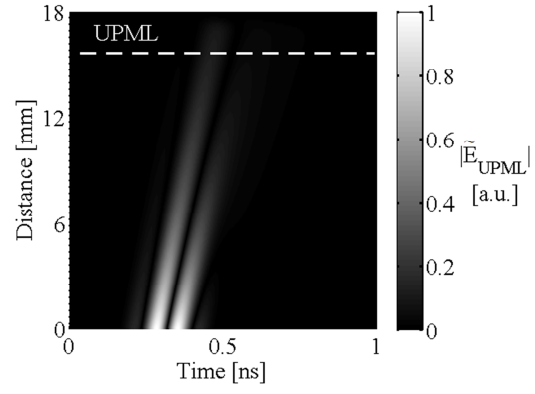
$$\mathbf{I}_s(t, z) = \exp\left\{-\left(\frac{t - T_c}{T_d}\right)\right\} \sin[2\pi f_e(t - T_c)] \delta(z - z_0) \hat{\mathbf{x}} \quad (43)$$

where  $T_d = 1/2.1f_e$ ,  $T_c = 4T_d$  and  $f_e = 6$  GHz given a spectral bandwidth of about 10 GHz. In this case, the time and spatial steps in the FDTD-based computations are  $\Delta t = 0.4$  ps and  $\Delta z = 0.7$  mm, respectively.

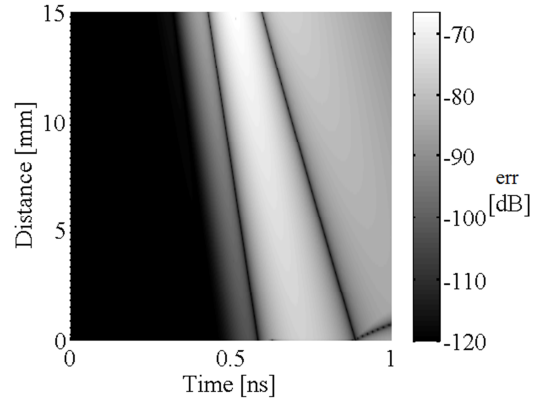
The computational domain has been bounded with UPML having electric conductivity profile and thickness carefully selected to minimize the spurious reflections. Fig. 2 shows the computed space–time distribution of the electric field, normalized with respect to the maximum value computed without



(a)



(b)



(c)

Figure 2: (a) Space-time electric field distribution without UPML and with a PEC boundary condition, (b) with UPML having  $d_{UPML} = 30\Delta z$ , (c) relative error.

UPML, by (a) neglecting UPML and terminating the computational domain with a PEC boundary condition, and (b) implementing the UPML with thickness  $d_{UPML} = 30\Delta z$ . By considering the reflected waves due to the PEC boundary condition, in Fig. 2(a) the spatial width has been chosen in order to ensure the absence of this kind of waves within the computational domain. Moreover, Fig. 2(c) shows the relative error (in dB) defined by the equation

$$\text{err} = 10 \log \left| \tilde{E}_0 - \tilde{E}_{UPML} \right|^2 \quad (44)$$

where  $\tilde{E}_0$  and  $\tilde{E}_{UPML}$  are the normalized electric field without and with UPML, respectively. The best calculated UPML settings are:  $\kappa_{MAX} = 1$ ,  $m = 7$ ,  $d_{UPML} = 30\Delta z$  and  $\sigma_{MAX} = 0.08(d_{UPML} + 1)/377\Delta z\epsilon_{rs}$ . By an inspection of Fig. 2(c), it is worthwhile to note the good performance of the UPML.

To validate the performance of the proposed FDTD scheme, the amplitudes of the electric field calculated in a CC, CD and HN media, characterized by the parameters reported in 1, are compared to their analytical values given by [16]

$$E(z + z^*, \omega) = E(z, \omega)T(z^*, \omega) \quad (45)$$

where the transfer function is

$$T(z^*, \omega) = \exp\{\gamma(\omega)z^*\} \quad (46)$$

and the complex wave number is

$$\gamma(\omega) = \gamma'(\omega) - j\gamma''(\omega) = j\frac{\omega}{c_0}\sqrt{\epsilon_r(\omega)} \quad (47)$$

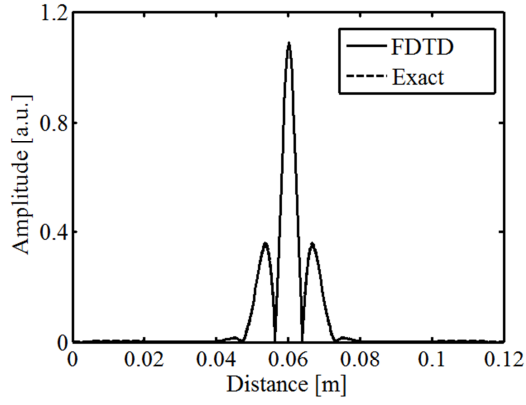
Fig. 3 depicts the spatial distribution of the electric field, at the time instant  $t = 0.3 \text{ ns}$ , considering a current source located in  $z_0 = 6 \text{ cm}$  for all the three

media. It can be seen that our FDTD results exhibit excellent agreement with the exact solution regarding the CC medium (see Fig. 3(a)). In fact, the FDTD results are essentially indistinguishable from exact ones. Moreover, both Figs. 3(b) and 3(c) illustrate the good accuracy of the proposed FDTD scheme for CD and HN media. In these cases, the FDTD results are slightly less accurate around the regions of local maxima. As result, it is possible to conclude that the new method presented herein is very accurate.

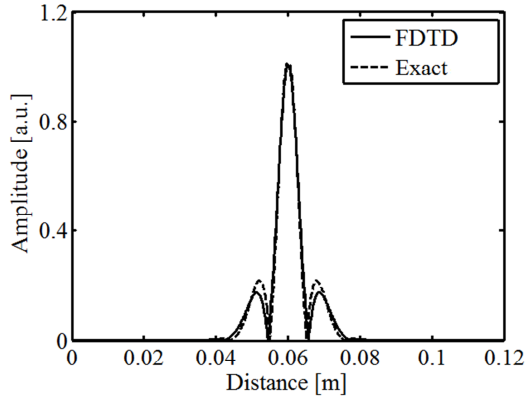
In the second example, the electromagnetic propagation within air/HN medium/air stratified system has been simulated. In particular, the reflection coefficient at the air/HN medium interface and the transmission coefficient at the HN medium/air interface have been calculated. In the simulations, the aforementioned Havriliak–Negami medium, density current source, time step and grid spacing have been taken into account.

The calculated numerical results versus the HN medium thickness are illustrated in Fig. 4. By an inspection of Fig. 4(a) it can be noted an evident resonance effect due to multiple internal reflections for frequencies  $f = 5$  GHz and  $f = 10$  GHz. For  $f = 1$  GHz this phenomenon is not relevant because the phase variation due to the thickness change is negligible. Moreover, for the frequency  $f = 10$  GHz the higher order internal reflections exhibit strong losses. As result, a quite constant reflection coefficient value of about 0.63 occurs for HN medium thickness higher than 15 mm.

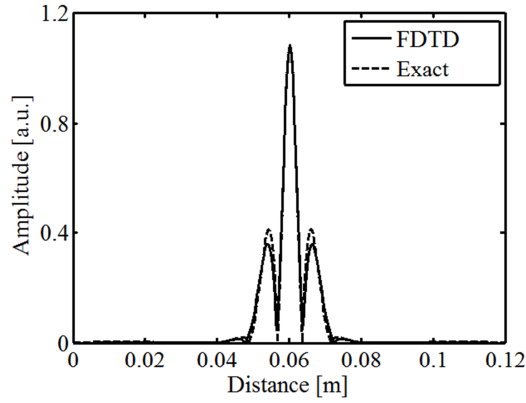
The FDTD results illustrated in Fig. 4(b) show a monotone decrease of the transmittance versus the HN medium thickness for all the three frequencies. Moreover, higher frequency signal components undergo a stronger attenuation. This effect can be explained by considering that the penetration



(a)



(b)



(c)

Figure 3: Spatial distribution of electric field in (a) Cole–Cole medium, (b) Cole–Davidson medium and (c) Havriliak–Negami medium derived from analytical approach (dashed line) and FDTD method (full line).



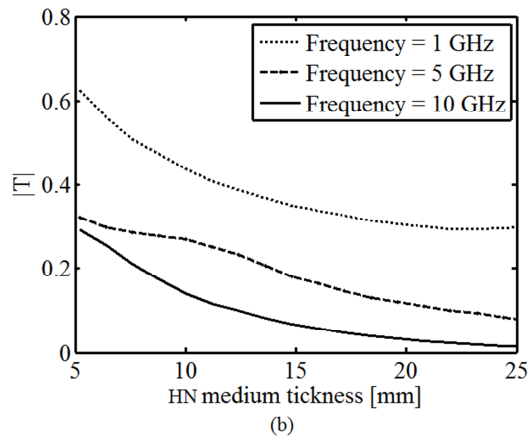
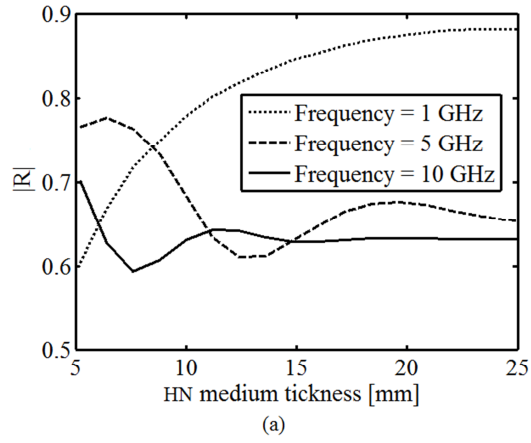


Figure 4: (a) Reflection coefficient amplitude and (b) transmission coefficient amplitude versus the HN medium thickness for three different frequencies: 1 GHz (dotted line), 5 GHz (dashed line), 10 GHz (full line).

depth decreases with the operating frequency. However, the reduced transmittance at 10 GHz, where the thickness of the HN dielectric slab is larger than 20 mm can be explained by taking into account that in this condition the penetration depth is much smaller than medium thickness.

Based on results illustrated in Fig. 4 we conclude that the proposed FDTD scheme is a useful computational tool for electromagnetic characterization of complex dispersive materials, such as biological tissues in radiofrequency domain.

#### 4. Conclusion

A new FDTD formulation for the solution of electromagnetic field propagation inside general dispersive media described by empirical Havriliak–Negami model has been presented. The method is based on the use of Riemann–Louville fractional operator theory and has been developed in order to approximate fractional derivatives using finite difference. The main feature of the proposed algorithm is the direct incorporation into the FDTD scheme of the fractional part of the dispersive permittivity function, which result in avoiding a number of auxiliary differential equations. Moreover, a dedicated UPML boundary condition formulation has been developed in order to take into account the Havriliak–Negami fractional response function. By comparing the FDTD results with those calculated by means of a fully analytical model it can be inferred that the proposed algorithm gets excellent accuracies in a wide frequency range. Moreover, the outstanding agreement between the analytical and the FDTD results indicates that the scheme does not exhibit significant numerical dispersion. The obtained numerical results

demonstrate that the proposed FDTD scheme allows a reliable electromagnetic field simulation within bulk and stratified complex dispersive materials as well as it could be used for electromagnetic characterization of biological tissues.

## References

- [1] A. T. Esser, K. C. Smith, T. R. Gowrishankar, J. C. Weaver, Towards solid tumor treatment by nanosecond pulsed electric fields, *Technology in Cancer Research and Treatment* 8 (2009) 289–306.
- [2] S. J. Beebe, Bioelectrics in basic science and medicine: Impact of electric fields on cellular structures and functions, *J. Nanomed. Nanotechol.* 4 (2013) 1000163.
- [3] R. Nuccitelli, U. Pliquett, X. Chen, W. Ford, R. J. Swanson, S. J. Beebe, J. F. Kolb, K. H. Schoenbach, Nanosecond pulsed electric fields cause melanomas to self-destruct, *Biochem Biophys Res Commun.* 343 (2006) 351–360.
- [4] J. Teissi, J. M. Escoffre, M. P. Rols, M. Golzio, Time dependence of electric field effects on cell membranes. a review for a critical selection of pulse duration for therapeutical applications, *Radiol. Oncol.* 42 (2008) 196–206.
- [5] S. Beebe, P. Fox, L. Rec, K. Somers, R. Stark, K. Schoenbach, Nanosecond pulsed electric field (nspef) effects on cells and tissues: Apoptosis induction and tumor growth inhibition, *IEEE Trans. Plasma Sci.* 30 (2002) 286–292.

- [6] F. Guo, C. Yao, C. Li, Y. Mi, Y. Wen, J. Tang, Dependence on pulse duration and number of tumor cell apoptosis by nanosecond pulsed electric fields, *IEEE Trans. Dielectr. Electr. Insul.* 20 (2013) 1195–1200.
- [7] R. Magin, *Fractional Calculus in Bioengineering*, Addison-Wesley, Begell House Publishers, 2006.
- [8] A. Taflov, S. Hagness, *Computational electrodynamics: the finite-difference time-domain method*, Artech House, Norwood, MA, 2005.
- [9] D. Caratelli, A. Yarovoy, A. Massaro, A. Lay-Ekuakille, Design and full-wave characterization of piezoelectric microneedle antenna sensors for enhanced near-field detection of skin cancer, *PIER* 125 (2012) 391–413.
- [10] D. Caratelli, A. Massaro, R. Cingolani, A. Yarovoy, Accurate time-domain modeling of reconfigurable antenna sensors for non-invasive melanoma skin cancer detection, *J. Sensors* 12 (2012) 635–643.
- [11] M.-R. Tofghi, FDTD modeling of biological tissues Cole-Cole dispersion for 0.530 GHz using relaxation time distribution samples—novel and improved implementations, *IEEE Trans. Microw. Theory Tech.* 57 (2009) 2588–2596.
- [12] W.-J. Chen, W. Shao, B.-Z. Wang, ADE-Laguerre-FDTD method for wave propagation in general dispersive materials, *IEEE Microw. Wireless Compon. Lett.* 23 (2013) 228–230.
- [13] I. T. Rekanos, FDTD schemes for wave propagation in Davidson-Cole dispersive media using auxiliary differential equations, *IEEE Trans. Antennas Propag.* 60 (2012) 1467–1478.

- [14] I. T. Rekanos, T. G. Papadopoulos, FDTD modeling of wave propagation in Cole-Cole media with multiple relaxation times, *IEEE Antennas Wireless Propag. Lett.* 9 (2010) 67–69.
- [15] H. H. Abdullah, H. A. Elsadek, H. E. ElDeeb, N. Bagherzadeh, Fractional derivatives based scheme for FDTD modeling of nth-order ColeCole dispersive media, *IEEE Antennas Wireless Propag. Lett.* 11 (2012) 281–284.
- [16] I. T. Rekanos, FDTD modeling of Havriliak-Negami media, *IEEE Microw. Wireless Compon. Lett.* 22 (2012) 49–51.
- [17] Z. Lin, On the FDTD formulations for biological tissues with Cole-Cole dispersion, *IEEE Microw. Wireless Compon. Lett.* 20 (2010) 244–246.
- [18] S. Su, W. Dai, D. T. Haynie, N. Simicevic, Use of the z-transform to investigate nanopulse penetration of biological matter, *Bioelectromagnetics* 26 (2005) 389–397.
- [19] B. Guo, J. Li, H. Zmuda, A new FDTD formulation for wave propagation in biological media with ColeCole model, *IEEE Microw. Wireless Compon. Lett.* 16 (2006) 633–635.
- [20] F. Torres, P. Vaudon, B. Jecko, Application of fractional derivatives to the FDTD modelling of pulse propagation in a Cole-Cole dispersive medium, *Microw. and Opt. Technol. Lett.* 13 (1996) 300–304.